Inorganic Chemistry

ARTICLE

pubs.acs.org/IC

Iron Salts with the Tetracyanidoborate Anion: $[Fe^{III}(H_2O)_6][B(CN)_4]_3$, Coordination Polymer $[Fe^{II}(H_2O)_2\{\kappa^2N[B(CN)_4]\}_2]$, and $[Fe^{II}(DMF)_6][B(CN)_4]_2$

Christian Nitschke and Martin Köckerling*

Institute of Chemistry, Inorganic-Solid State Chemistry Group, University of Rostock, Albert-Einstein-Strasse 3a, D-18059 Rostock, Germany

ABSTRACT: The reaction of $Fe(OH)_3$ with tetracyanidoboronic acid, $H[B(CN)_4]\cdot xH_2O$, in water leads to the first examples of tetracyanidoborates with a triply charged metal cation, $[Fe^{III}(H_2O)_6][B(CN)_4]_3$ (**1**). Using elemental iron powder as starting material, $[Fe^{II}(H_2O)_2\{\kappa^2NB(CN)_4]\}_2]$ (**2**) is obtained. Anhydrous iron(II) tetracyanidoborate, which is synthesized by heating of **2**, is soluble in dry dimethylformamide. After evaporation of the DMF solvent, single crystals of the third title compound, $[Fe^{II}(DMF)_6][B(CN)_4]_2$ (**3**), are obtained. Compound **3** is the first metal tetracyanidoborate soluble in nonpolar solvents. The title compounds have been characterized by single-crystal X-ray diffraction (**1** rhombohedral, $R\bar{3}c$ (no. 167), a = 14.9017(7) Å, c = 20.486(1) Å, Z = 6; **2** tetragonal, $I\bar{4}2d$ (no. 122), a = 12.3662(3) Å, c = 9.2066(4) Å, Z = 4; **3** triclinic, $P\bar{1}$ (no. 2), a = 8.6255(3) Å, b = 11.0544(4) Å, c = 12.2377(5) Å, Z = 1). The metal ions in all three compounds are octahedrally coordinated. Whereas **1** and **3** are built up from isolated complex ions, **2** comprises a coordination polymer, in which the Fe^{II} ion is coordinated by two oxygen atoms of two water molecules in a trans orientation and four nitrogen donor atoms of the $[B(CN)_4]^-$ groups, which bridge between neighboring iron ions. The iron(III) ion in **3** is in a perfect octahedral environment, which is formed by the O atoms of 6 molecules of water. The single-crystal X-ray structures, vibrational spectra, thermal properties, solubilities, and electrochemical characteristics are reported and compared with those of other known tetracyanidoborates.

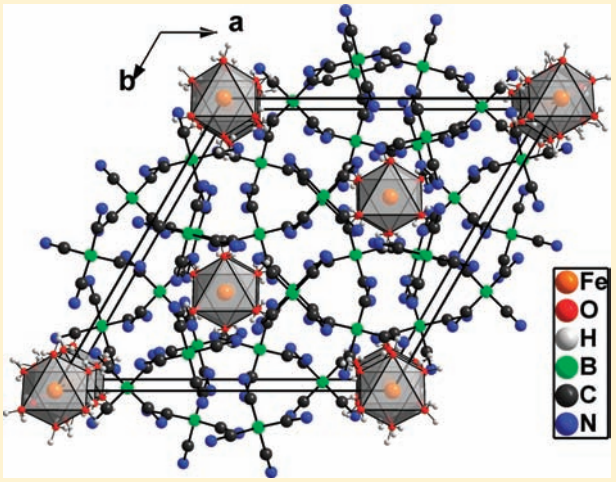

INTRODUCTION

Even though the first attempts to synthesize the tetracyanidoborate anion were reported already in 1951[1] the first X-ray crystal structures of tetracyanidoborate salts were published not before the year 2000.[2,3] After an improvement of the synthetic procedure in 2003, a molten flux reaction of KCN with KBF_4 in LiCl, which makes tetracyanidoborates accessible in multigram amounts,[4] the chemistry of tetracyanidoborates has been developed rapidly. Since then salts with the $[B(CN)_4]^-$ anion are attracting increasing scientific and commercial interest. The main reasons for this development are the unique properties of the tetracyanidoborate anion, which is chemically robust but weakly coordinating. Because of these properties, $[B(CN)_4]^-$-containing salts have found applications as starting materials for the synthesis of new unusual materials, like $[B(CF_3)_4]^-$- or $[B(CN)_4\cdot(B(C_6F_5)_3)_4]^-$-containing salts, which are able to stabilize new highly reactive cations.[2b,5−7] Ionic liquids with the tetracyanidoborate anion have large electrochemical windows and low viscosities and are useful, for example, in solar cells.[8] They have also found applications as components of membranes, used in selective separation procedures.[9] Many tetracyanidoborate salts crystallize in fascinating network structures, of which a series of compounds with monovalent and divalent cations have been published so far.[10−15]

In this article, the syntheses, X-ray structures, thermochemical properties, electrochemical characteristics, and vibrational spectra of the first examples of iron tetracyanidoborates $[Fe^{III}(H_2O)_6][B(CN)_4]_3$ (**1**), the coordination polymer $[Fe^{II}(H_2O)_2\{\kappa^2NB(CN)_4]\}_2]$ (**2**), and $[Fe^{II}(DMF)_6][B(CN)_4]_2$ (DMF = dimethylformamide) (**3**) are presented and compared with other known tetracyanidoborates with singly or doubly charged counterions. Compound **1** is the first tetracyanidoborate with a triply charged metal cation.

EXPERIMENTAL SECTION

Materials. All starting materials were used as received from commercial sources with purities higher than 97%. Tetracyanidoboronic acid was obtained through an ion-exchange process according to ref 11 by

Received: November 12, 2010
Published: April 13, 2011

ACS Publications © 2011 American Chemical Society

Table 1. Crystal Data and Structure Refinement Parameters for $[Fe(H_2O)_6][B(CN)_4]_3$, $[Fe(H_2O)_2\{\kappa^2N[B(CN)_4]\}_2]$, and $[Fe(DMF)_6][B(CN)_4]_2$

	$[Fe(H_2O)_6][B(CN)_4]_3$	$[Fe(H_2O)_2\{\kappa^2N[B(CN)_4]\}_2]$	$[Fe(DMF)_6][B(CN)_4]_2$
formula	$C_{12}H_{12}B_3FeN_{12}O_6$	$C_8H_4B_2FeN_8O_2$	$C_{26}H_{42}B_2FeN_{14}O_6$
fw (g/mol)	508.62	319.65	724.21
T (K)	173(2)	90(2)	173(2)
cryst syst	rhombohedral	tetragonal	triclinic
space group	$R\bar{3}c$ (no. 167)	$I\bar{4}2d$ (no. 122)	$P\bar{1}$ (no. 2)
Z	6	4	1
a (Å)	14.9017(7)	12.3662(3)	8.6255(3)
b (Å)	14.9017(7)	12.3662(3)	11.0544(4)
c (Å)	20.486(1)	9.2066(4)	12.2377(5)
α (deg)	90	90	65.987(2)
β (deg)	90	90	75.521(2)
γ (deg)	120	90	76.639(2)
V (Å^3)	3939.6(3)	1407.90(8)	1020.93(7)
ρ_{calcd} (g·cm^{-3})	1.286	1.508	1.178
μ (mm^{-1})	0.622	1.085	0.421
λ (Å)	0.71073	0.71073	0.71073
no, of params	61	49	224
Gof on F^2	1.109	0.991	1.052
R indices $[I > 2\sigma(I)]$	$R1 = 0.0199$, $wR2 = 0.0654$	$R1 = 0.0329$, $wR2 = 0.0690$	$R1 = 0.0341$, $wR2 = 0.083$
weighting A/B[c]	0.0070/3.3647	0.0498/4.6930	0.0374/0.27

[a] $R1 = \Sigma||F_o| - |F_c||/\Sigma|F_c|$. [b] $wR2 = ([\Sigma\{w(F_o^2 - F_c^2)^2\}/\Sigma\{w(F_o^2)^2\}])^{1/2}$. [c] $w = 1/[(\sigma^2(F_o^2) + (A\cdot P)^2 + B\cdot P]$; $P = (F_o^2 + 2F_c^2)/3$.

rinsing a solution of $K[B(CN)_4]$ slowly through a column, which is filled with the strong acidic cation exchanger Lewatit S100 (Bayer AG), which was previously treated with 1 mol·L^{-1} HCl. The concentration of the obtained $H[B(CN)_4]$ solution was 0.23 mol·L^{-1}. Potassium tetracyanidoborate was synthesized according to ref. 4 by a high-temperature treatment of a solid mixture of LiCl, KCN, and $K[BF_4]$ (molar ratio of 9:9:1) followed by a purification process. The hydroxide $Fe(OH)_3$ was precipitated from an aqueous solution of $FeCl_3\cdot 6H_2O$ with concentrated NH_3. The solid hydroxide was filtered off and dissolved in the tetracyanidoboronic acid immediately after precipitation to prevent altering to the oxide. The used dimethylformamide was distilled and dried with the aid of molecular sieves (3 Å) before use.

Safety Notes! Cyanides are highly toxic, especially if dissolved in organic solvents. On contact with acidic materials they can evolve highly toxic HCN gas. They must always be handled with sufficient precaution.

Synthesis of $[Fe^{III}(H_2O)_6][B(CN)_4]_3$ (1). The iron(III) tetracyanidoborate, **1**, was synthesized by a reaction of $Fe(OH)_3$ as starting material with $H[B(CN)_4]$. In a 50 mL round-bottomed flask, freshly precipitated $Fe(OH)_3$, obtained from treatment of a solution of $FeCl_3\cdot 6H_2O$ in water with NH_3, is added in small portions to 10 mL of a 0.23 M solution of $H[B(CN)_4]$ (2.3 mmol). The mixture was stirred with a magnetic stirring bar under continuous control of the pH value. The reaction was considered to be completed and addition of $Fe(OH)_3$ was stopped, when the pH reached 7.0. The solution was filtered to separate any undissolved material from the clear colorless solution. The solvent was slowly evaporated at room temperature, and colorless single crystals were obtained, which were suitable for a single-crystal X-ray structure determination. The yield of $[Fe(H_2O)_6][B(CN)_4]_3$ was 0.36 g (93%). Anal. Calcd for $C_{12}H_{12}B_3FeN_{12}O_6$ (M = 504.7 g·mol^{-1}): C, 28.34; N, 33.05; H, 2.38. Found: C, 28.58; N, 32.64; H, 2.18. IR (ATR, cm^{-1} ν_{max}): 2966, 2410, 1615, 951, 933, 842, 635. Raman (cm^{-1} ν_{max}): 2254, 2246, 950, 941, 931, 532, 518, 510, 334, 170, 152, 137, 125, 119, 107, 83, 66.

Synthesis of $[Fe(H_2O)_2\{\kappa^2N[B(CN)_4]\}_2]$ (2). The iron(II) tetracyanidoborate, **2**, was synthesized by using elemental iron powder as starting material. In a 50 mL round-bottomed flask 82 mg (1.47 mmol) of iron powder was added in small portions to 11.5 mL of 0.23 M $H[B(CN)_4]$ (2.65 mmol). To accelerate the reaction, the mixture was slightly heated and an evolution of hydrogen gas was observed. Undissolved iron powder was removed with the aid of a bar magnet from the light yellowish clear solution. The reaction was considered to be completed when the pH value reached 7.0. The solvent was slowly evaporated at room temperature, and light green single crystals were obtained, which were suitable for a single-crystal X-ray structure determination. The yield of $[Fe(H_2O)_2\{\kappa^2N[B(CN)_4]\}_2]$ was 0.4 g (95%). Anal. Calcd for $C_8B_2N_8H_4O_2Fe$ (M = 321.64 g·mol^{-1}): C, 29.87; N, 34.84; H, 1.25. Found: C, 29.43; N, 34.73; H, 1.21. IR (ATR, cm^{-1} ν_{max}): 3329, 3253, 2265, 2227, 1652, 985, 948, 924, 851, 613, 538. Raman (cm^{-1} ν_{max}): 2264, 2225, 979, 936, 547, 520, 501, 231, 180, 111, 93.

Synthesis of $[Fe(DMF)_6][(B(CN)_4)]_2$ (3). $[Fe(DMF)_6][B(CN)_4]_2$ was synthesized by dissolving $Fe[B(CN)_4]_2$ in dry dimethylformamide. For this reaction 128 mg of $[Fe(H_2O)_2\{\kappa^2N[B(CN)_4]\}_2]$ was dried at 170 °C in an open glass tube in a tube furnace. After drying 114 mg (0.4 mmol) of the anhydrous material was obtained and dissolved in 0.5 mL (0.47 g, 6.43 mmol) of dry DMF in a 25 mL round-bottomed flask. The solvent was slowly evaporated at room temperature in a drybox, and colorless single crystals were obtained, which were suitable for a single-crystal X-ray structure determination. The yield of $[Fe(DMF)_6][(B(CN)_4)]_2$ was 0.282 g (97.4%). Anal. Calcd for $C_{26}B_2N_{14}H_{42}O_6Fe$ (M = 724.18 g·mol^{-1}): C, 43.12; N, 27.08; H, 5.85. Found: C, 42.78; N, 26.43; H, 6.11. IR (ATR, cm^{-1} ν_{max}): 2939, 2815, 2222, 1641, 1495, 1433, 1423, 1379, 1250, 1112, 1061, 955, 928, 865, 842, 682.

Structure Analysis and Refinement. Transparent single crystals of the title compounds for X-ray diffraction investigations were selected with the aid of a microscope. They were mounted on the tips of thin glass fibers for the single-crystal X-ray diffraction measurements. Data were collected on a Bruker-Nonius Apex X8 diffractometer, equipped with a CCD detector. Measurements were done using monochromatic Mo Kα radiation (λ = 0.71073 Å). Preliminary data of the unit cell were obtained from the reflex positions of 12 frames, each

dx.doi.org/10.1021/ic102278z |Inorg. Chem. 2011, 50, 4313–4321

measured in three different directions of the reciprocal space. After completion of the data measurements the intensities were corrected for Lorentz, polarization, and absorption effects using the Bruker-Nonius software.[16] The structures were solved by direct methods using the SHELXS-97 program and refined by least-squares procedures on F^2 with the aid of the SHELXL-97 program.[17] A X-ray crystallographic file of $[Fe(H_2O)_6][B(CN)_4]_3$ (**1**), $[Fe(H_2O)_2\{\kappa^2NB(CN)_4\}_2]$ (**2**), and $[Fe(DMF)_6][B(CN)_4]_2$ (**3**), in CIF format is available. This material is available free of charge via the CCDC data center, CCDC-420959 for **1**, CCDC-420958 for **2**, and CCDC-743432 for **3**.

All non-hydrogen atoms were refined anisotropically. The H atoms of **1** were located from difference Fourier maps and refined isotropically. Those of **2** and **3** were added on idealized positions and refined using riding models. Crystal data, data collection, and refinement parameters are compiled in Table 1.

Vibrational Spectroscopy. The IR spectra of $[Fe^{III}(H_2O)_6][B(CN)_4]_3$, $[Fe^{II}(DMF)_6][(B(CN)_4)]_2$, and $[Fe^{II}(H_2O)_2\{B(CN)_4\}_2]$ in the range of 4000−500 cm^{-1} were obtained with a Nicolet 380 FT-IR spectrometer with a Smart Endurance ATR device. Raman spectra were recorded at room temperature with a Bruker Vertex 70 Raman spectrometer (Bruker, Karlsruhe, Germany) by using the 1064 nm exciting line of a Nd/YAG laser. The crystalline samples were flame sealed in melting point capillaries.

DSC and TG Measurements. The differential scanning calorimetry (DSC) measurements have been carried out with a DSC 823e Mettler Toledo apparatus. The samples were heated to 600 °C. Thermogravimetry (TG) measurements have been carried out with a Setram Labsys thermal analyzer. The sample of $[Fe^{III}(H_2O)_6][B(CN)_4]_3$ was heated to 900 °C. Cyclic measurements were performed to prove reversibility. The heating rate for all measurements was 10 K/min.

Elemental Analysis. Elemental analyses were accomplished by a microanalytical combustion method with the Euro EA3000 instrument (HEKATech GmbH, Wegberg, Germany). The error margins for determination of the elements were C ± 0.3%, N ± 0.2%, and H ± 0.51%.

Solubilities. The solubilities of $[Fe(H_2O)_2\{\kappa^2N[B(CN)_4]\}_2]$ in methanol, water, and acetone were determined at 24 °C under atmospheric pressure. Saturated solutions of the title compounds in the respective solvents were placed in small glass vials. A precisely measured volume (about 1.0 mL) of each of the saturated solutions was transferred into a weighed empty glass container. The solvent was evaporated until the material was dry and the vials weighted again. The mass was measured again afterward and the solubility calculated. The solubilities of $[Fe^{III}(H_2O)_6][B(CN)_4]_3$ and $[Fe^{II}(DMF)_6][B(CN)_4]_2$ in various solvents have been determined qualitatively.

Electrochemical Measurements. Cyclovoltammetric measurements were carried out with Gamry Instruments (GI) "Dr. Bob's Cell for Small-Scale Electrochemistry" with the PCI4/300TM potentiostate and a platinum glass electrode as working electrode in a conventional three-electrode cell. A saturated calomel electrode was used as reference. Potentials are given relative to the NHE electrode. The Physical Electrochemisty Software PHE 200 (GI) was used for measuring and analyzing the cyclovoltammograms. Cyclovoltammetric measurements were carried out in 15 mmol·L^{-1} aqueous solutions with 0.1 mol·L^{-1} KPF_6 as electrolyte. Measured potentials were checked using an equimolar (15 mmol·L^{-1}) aqueous solution of $K_3[Fe(CN)_6]$ and $K_4[Fe(CN)_6]$ with the same amount of KPF_6 as standard.

RESULTS AND DISCUSSION

A. Synthetic Aspects. To date several methods have been developed to synthesize new tetracyanidoborates. All depend on the material, which is obtained by the necessary preceding step of the synthesis of the $[B(CN)_4]^-$ ion.[4] After the purification process $K[B(CN)_4]$ is obtained according to ref. 4 from which $[Et_3NH][B(CN)_4]$ can be easily prepared. New metal−tetracyanidoborates are accessible from this compound by reaction with strong bases, like LiOH or $Ca(OH)_2$. Starting from the potassium salt, metathesis reactions in solution or ion-exchange processes lead to new tetracyanidoborate salts. A third method involves the strong tetracyanidoboronic acid,[8] which can be obtained from the potassium salt. As strong acid, $H[B(CN)_4]$ can easily oxidize electropositive metals forming the corresponding salt of that metal.

Scheme 1. Reaction of Elemental Iron with Tetracyanidoboronic Acid

$$Fe_{(s)} + 2\ H[B(CN)_4]_{(aq)} + 2\ H_2O \longrightarrow [Fe^{II}(H_2O)_2\{\kappa^2N[B(CN)_4]\}_2] + H_{2(g)}$$

$[Fe(H_2O)_6][B(CN)_4]_3$. As described below, oxidation of elemental iron with $H[B(CN)_4]_{(aq)}$ leads to the iron(II) compound **2** and further oxidation to iron(III) is not observed. Therefore, the synthesis of **1** is achieved by the acid−base reaction of $Fe^{III}(OH)_3$ with tetracyanoboronic acid. The colorless compound $[Fe(H_2O)_6][B(CN)_4]_3$ is obtained from this solution after evaporation of the solvent in high purity and high yield (>90%).

$[Fe(H_2O)_2\{\kappa^2N[B(CN)_4]\}_2]$. This new compound has been synthesized by a reaction of tetracyanoboronic acid with elemental iron in aqueous solution according to Scheme 1.

Oxidation of the iron does not exceed the +2 oxidation state, and **2** is obtained in high yield, >90% ,and high purity.

$[Fe^{II}(DMF)_6][(B(CN)_4)]_2$. Dehydration of $[Fe^{II}(H_2O)_2\{\kappa^2N[B(CN)_4]\}_2]$ at 170° leads (presumably) to $Fe[B(CN)_4]_2$ (see below, Thermochemical Properties), which is not soluble in most common solvents (acetonitrile, ethanol, methanol, tetrahydrofuran, dichloromethane, and acetone). Exceptions are the very polar solvents dimethylformamide (DMF) and dimethylsulfoxide (DMSO). By dissolving $Fe[B(CN)_4]_2$ in an excess of DMF and evaporation of the excess solvent $[Fe^{II}(DMF)_6][(B(CN)_4)]_2$ is obtained in high yield (>90%).

B. Thermochemical Properties. *$[Fe^{III}(H_2O)_6][B(CN)_4]_3$.* Combined DSC and thermogravimetric measurements have been carried out on $[Fe^{III}(H_2O)_6][B(CN)_4]_3$ in the temperature range from 25 to 900 °C. The compound is thermally stable up to 155 °C (onset). From that temperature on up to 200 °C an endothermic event happens that is accompanied by a mass loss of 25%. This is more than thermal dehydration would give, which is only 21%. A second endothermic peak at 277 °C (onset) is followed by two exothermic peaks at 590 and 686 °C. It is obvious that on heating a more complex chemical reaction happens than just thermal dehydration. Further investigations are needed to find out more about the thermal behavior of $[Fe^{III}(H_2O)_6][B(CN)_4]_3$.

$[Fe^{II}(H_2O)_2\{\kappa^2N[B(CN)_4]\}_2]$. DSC measurements have been carried out on $[Fe^{II}(H_2O)_2\{\kappa^2N[B(CN)_4]\}_2]$ also in the temperature range from 25 to 600 °C. A complete loss of the coordinated water molecules happens between 133 and 155 °C at ordinary pressure with a dehydration enthalpy of 116.4 kJ·mol^{-1}. A 200 mg amount of $[Fe^{II}(H_2O)_2\{\kappa^2N[B(CN)_4]\}_2]$ has been exposed to a temperature of 170 °C for 1 h to prove complete loss of water at this temperature. The found mass loss was as expected, 22.4 mg (11.2%). Table 2 compares the dehydration and decomposition temperatures and dehydration enthalpies of $[Fe^{II}(H_2O)_2\{\kappa^2N[B(CN)_4]\}_2]$, $[Zn^{II}(H_2O)_2\{\kappa^2N[B(CN)_4]\}_2]$,[18] and $[Co^{II}(H_2O)_2\{\kappa^2N[B(CN)_4]\}_2]$.[13]

Table 2. Dehydration and Decomposition Temperatures (onset temperatures) and Dehydration Enthalpies of $[Fe^{II}(H_2O)_2\{\kappa^2N[B(CN)_4]\}_2]$, $[Zn^{II}(H_2O)_2\{\kappa^2N[B(CN)_4]\}_2]$, and $[Co^{II}(H_2O)_2\{\kappa^2N[B(CN)_4]\}_2]$

compound	dehydration temp./°C	dehydration enthalpy/kJ·mol^{-1}	decomposition temp./°C
$[Co^{II}(H_2O)_2\{\kappa^2N[B(CN)_4]\}_2]$	108−130	89.2	510
$[Zn^{II}(H_2O)_2\{\kappa^2N[B(CN)_4]\}_2]$	110−130	100.4	473
$[Fe^{II}(H_2O)_2\{\kappa^2N[B(CN)_4]\}_2]$	133−155	116.4	550

The dehydration enthalpy increases from the cobalt and zinc to the iron compound. This trend is also visible in the dehydration temperatures. These compounds can as well be dehydrated at reduced pressure (15 mbar) at 40 °C. $[Fe^{II}(H_2O)_2\{\kappa^2N[B(CN)_4]\}_2]$ starts to decompose at 550 °C without previous melting. The reason for this behavior can be seen in the higher lattice energy compared to the tetracyanidoborates with monovalent cations, which melt before decomposing.[10b]

$[Fe^{II}(DMF)_6][B(CN)_4]_2$. When crystals of **3** are separated from the DMF solution, they loose within minutes at room temperature two molecules of the coordinated DMF ligands. Elemental analysis of the resulting compound $C_{20}B_2N_{12}H_{28}O_4Fe$ (that is, $[Fe^{II}(DMF)_4][B(CN)_4]_2$, M = 577.99 g·mol^{-1}) is as follows: C, 41.56; N, 29.08; H, 4.88. Found: C, 40.63; N, 29.49; H, 4.67%). At 1 mbar and 45 °C two further molecules of DMF are removed. (Anal. Calcd for $C_{26}B_2N_{14}H_{42}O_6Fe$ (=$[Fe^{II}(DMF)_2][B(CN)_4]_2$, M = 431.8 g·mol^{-1}): C, 38.94; N, 32.44; H, 3.27. Found: C, 38.81; N, 31.64; H, 3.59%. These two steps of loosing coordinated DMF molecules are not observed in the DSC curve; instead, they show in the temperature range from 25 to 600 °C a sharp endothermic peak at 80 °C (onset). By heating the compound with the aid of a Boetius apparatus, the melting point has been detected at 84 °C. Thus, the endothermic effect at 80 °C in the DSC corresponds to the melting point. The DSC curve shows a second endothermic peak at 250 °C (onset). At this temperature crystal formation has been observed. It is likely that the remaining coordinated DMF molecules vaporize at 250 °C and leave the solvent-free compound $Fe[B(CN)_4]_2$, which crystallizes. Exothermic decomposition takes place at the same temperature as that found for compound **2** (550 °C).

C. Spectroscopic Aspects. From samples of all three title compounds IR and Raman spectra were recorded. Comparing the IR with the Raman spectra shows that bands originating from the same molecular vibrations appear in both spectra almost at the same frequency. Complete analysis of the spectrum of the $[B(CN)_4]^-$ ion is given in ref 2a. The CN stretching mode of **1** is only visible in the Raman spectrum. In the IR spectrum it is hidden by a broad band originating from OH vibrations. In the Raman spectra of compounds **1** and **2** and in the IR spectrum of **2** the CN stretching mode is separated into two bands. This band is not expected in the IR spectrum but appears with weak intensity because of the deviation of the shape of the $[B(CN)_4]^-$ from ideal tetrahedral (see structural discussion, below). In $[Fe^{II}(H_2O)_2\{\kappa^2N[B(CN)_4]\}_2]$ the band at 2265 cm^{-1} originates from the coordinated cyanide groups and at 2227 cm^{-1} from the noncoordinated ones. The wavenumber of the CN stretching mode is correlated with the strength of the bonding interaction of the cyanide groups with the metal.[10b,c] It decreases from the Cu (2291 cm^{-1}), Zn (2279 cm^{-1}), Co (2275 cm^{-1}), and Fe (2265 cm^{-1}) to the Hg compound (2264 cm^{-1}). For $[Fe^{III}(H_2O)_6][B(CN)_4]_3$ a separation of the CN stretching modes into two bands (2246 and 2254 cm^{-1}) is observed also. In contrast to that of compound **2** this separation cannot be explained by different direct coordination of the CN groups to the metal ions. The reason can be seen in different linkage of the cyanide groups with the water molecules through hydrogen bonds. The different distances between the oxygen atoms of the iron surrounding water molecules and the cyanido nitrogen atoms (N1···O1 2.748(1) Å and N2···O1 2.707(1) Å) cause hydrogen bonds of different strength. Because of the same number of the two different distances the CN stretching mode is separated symmetrically in a ratio of 1:1. The higher wavenumber can be assigned to the shorter hydrogen bond because of stronger interaction.[10b,c] They are slightly lower than that of the coordinated groups in the divalent compounds but higher than that of the noncoordinated ones. They can be compared with the wavenumbers of the CN streching in monovalent tetracyanidoborates,[10b] which shows that there is a remarkable interaction between the cyanido groups and the water molecules, which is increased through the Lewis-acidic iron(III) ion.

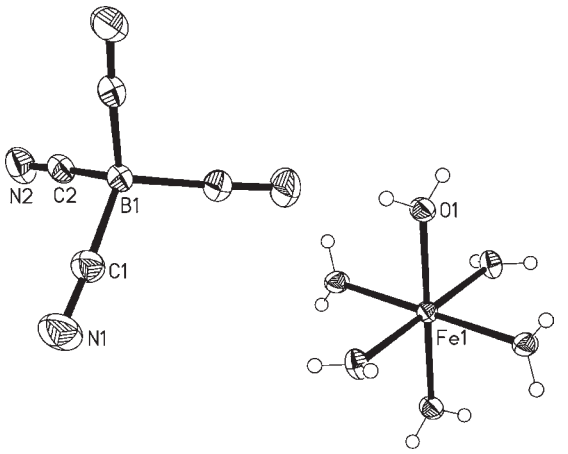

Figure 1. View of the molecular structures of the isolated $[Fe(H_2O)_6]^{3+}$ cation and the $[B(CN)_4]^-$ anion in crystals of $[Fe(H_2O)_6][B(CN)_4]_3$ (thermal displacement ellipsoids at the 50% probability level).

Whereas in the IR spectrum of **2** the CN stretching mode is weak, that of **3** is of medium intensity. Raman spectra of **3** could not be recorded, because the compound decomposes under the influence of the laser light. Because of weak ionic interactions between the $[Fe^{II}(DMF)_6]^{2+}$ cation and the tetracyanidoborate anion the IR spectrum of $[Fe^{II}(DMF)_6][B(CN)_4]_2$ shows only one CN band at 2222 cm^{-1}. This value compares well with the wavenumber found, for example, in $[Bu_4N][B(CN)_4]$ or $(BMIm)[B(CN)_4]$ (BMIm, 1-butyl-3-methyl-imidazolium).[10b] The CO stretching mode of the DMF molecules can be assigned to the band at 1641 cm^{-1} in the IR spectrum, which is lower than that in free DMF molecules (1687 cm^{-1})[19] due to the coordination of the DMF oxygen atoms to the iron(II) ion. The result is a weakened CO bond and hence a lower wavenumber. In $[Mg(DMF)_6][B(CN)_4]_2$ and $[Zn(DMF)_6][B(CN)_4]_2$ the CO

dx.doi.org/10.1021/ic102278z |*Inorg. Chem.* 2011, 50, 4313–4321

Table 3. Selected Atom Distances (Å) within $[Fe(H_2O)_6][B(CN)_4]_3$, $[Fe(H_2O)_2\{\kappa^2N[B(CN)_4]\}_2]$, and $[Fe(DMF)_6][B(CN)_4]_2$

	$[Fe(H_2O)_2\{\kappa^2N[B(CN)_4]\}_2]$	$[Fe(H_2O)_6][B(CN)_4]_3$	$[Fe(DMF)_6][B(CN)_4]_2$
cation			
Fe−O	2.072(1)	1.9891(6)	2.098(1)-2.119(1)
average			2.110
Fe−N	2.168(2)		
anion			
B−C	1.599(3)−1.601(3)	1.5905(9)−1.592(1)	1.586(3)−1.593(3)
average	1.600	1.5914	1.590
C−N	$1.143(3)_{coordinated}$	1.139(1)−1.140(1)	1.135(2)−1.138(2)
	$1.149(3)_{noncoordinated}$		
average		1.140	1.136

stretching modes are detected at 1654 and 1644 cm^{-1}.[18] This trend correlates with the Lewis acid strength of the metal ion. The other modes of the coordinated DMF molecule are nearly similar to those of the free solvent molecules. Those which are affected by the coordination to the iron(II) ion can be found at slightly lower wavenumbers than in the noncoordinated DMF molecules.

D. Electrochemical Properties. Cyclovoltammetric measurements have been carried out on aqueous solutions of compounds **1** and **2**. Reduction of the iron(III) tetracyanidoborate to the iron(II) compound is observed at a half-wave potential of 711 mV ($\varphi_P{}^a$ = 632 mV; $\varphi_P{}^k$ = 790 mV). The symmetric shape of the anodic and cathodic peaks and the same currents in the CV of **1** indicates a reversible redox process, even though the separation of the peaks is larger than theoretically expected. However, about the same difference is observed for the used standard redox couple, the Fe^{II}/Fe^{III} prussiates. Irreversible conversion of the iron(II) compound to elemental iron is observed in the negative voltage range at $\varphi_P{}^a$ = −292 mV and $\varphi_P{}^k$ = −79 mV. Also, a reversible Fe^{II}/Fe^{III} redox process is found for $[Fe(H_2O)_2\{\kappa^2NB(CN)_4\}_2]$ at the half-wave potential of 684 mV. The value of +711 mV for the half-wave potential compares well with the standard potential for the Fe^{III}/Fe^{II} couple of +771 mV, for which the hydrated species can be assumed.[20] Therefore, it is interesting to see that the half-wave potential of **2** is more negative than for **1**, indicating that in solution the coordination environment of the Fe^{II} ion of **2** is not the same as that of the Fe(III) ion of **1**, i.e., not completely hydrated. It can be assumed that the coordination environment still contains some CN groups, which is supported by the fact the hexacyanido complexes of the Fe^{III}/Fe^{II} couple have a more negative half-wave potential than the hydrated couple (+358 mV).

E. Structural Aspects. *$[Fe(H_2O)_6][B(CN)_4]_3$.* Colorless single crystals of compound **1** were obtained after slow evaporation of the solvent (water) at room temperature of a saturated solution and after filtering off excess $Fe(OH)_3$. $[Fe(H_2O)_6][B(CN)_4]_3$ crystallizes very similar to $[Cr(H_2O)_6]Cl_3$ (or $[Al(H_2O)_6]Cl_3$),[21] in the rhombohedral space group $R\bar{3}c$ (no. 167). Also, the crystal structure of the iron(II) perchlorate hydrate, $[Fe(H_2O)_6][ClO_4]_3 \cdot 3H_2O$, shows close similarities to **1**, besides the fact that additional cocrystallized water molecules are present.[22a] The structure contains isolated $[Fe(H_2O)_6]^{3+}$ cations and $[B(CN)_4]^-$ anions. In the cation the Fe^{3+} ion is perfectly octahedrally surrounded by 6 molecules of water and three tetracyanidoborate anions per metal cation. Figure 1 shows the coordination environment of the Fe^{3+} ion and the molecular structure of the tetracyanidoborate anion. The iron(III) ion is located on a site with $\bar{3}$ symmetry (Wyckoff site 6b of the space group $R\bar{3}c$). Thereby, all Fe−O distances are of same length (1.9898(1) Å) and all O−Fe−O angles are 90°. Selected bond distances of **1** together with those of **2** and **3** are collected in Table 3 and selected bond angles in Table 4. The Fe−O bond length is in the same range as those in other iron(III) compounds with an octahedral coordination environment consisting of 6 water molecules.[22] The symmetry-independent tetracyanidoborate anion in **1** is located on the 18*e* Wyckoff site in $R\bar{3}c$ with 2-fold rotational symmetry. It is slightly distorted from ideal tetrahedral symmetry with C−B−C angles between 107.39(4)° and 111.55(9)°. The average B−C (1.592 Å) and C−N (1.140 Å) bond lengths are in good agreement with those in other tetracyanidoborates with doubly or singly charged cations.[10−15] Two different short distances of 2.707(1) and 2.748(1) Å exist between the symmetry-independent cyanido nitrogen atoms and water oxygen atoms resulting in hydrogen contacts of different strengths. Every N atom has a further, longer N···H−O contact (N1 3.281(1) Å and N2 3.260(1) Å) to the same $[Fe(H_2O)_6]^{3+}$ unit. The short distances correspond to relatively strong hydrogen bonds. The environment of the $[B(CN)_4]^-$ ion is shown in Figure 2. Assuming a pure ionic model of the AX_3 type an octahedrally coordinated cation A requires a coordination number of 2 for the X anion, as found, for example, in ReO_3. In **1**, which consists of more complex ionic units than ReO_3, not only two but every N atom of the $[B(CN)_4]^-$ anion forms strong H bonds to the water molecules of the $[Fe(H_2O)_6]^{3+}$ units (CN 4 in a first approximation). Therefore, the coordination number of the complex cation needs to be 12, which is actually found. Figure 3 gives a sketch of the coordination environment of the $[Fe(H_2O)_6]^{3+}$ ion. It can be described as distorted anticuboctahedral. Because of the above-mentioned hydrogen bonds a three-dimensional network structure of interconnected iron−water octahedra and tetracyanidoborate tetrahedra exists. Figure 4 gives a view along *c* of the content of the unit cell. The different strength of the hydrogen bonds is also visible in the Raman spectrum, where two CN absorption frequencies are observed (see Vibrational Spectroscopy) in accordance with the two different (short) N···H−O contacts of each CN group.

$[Fe(H_2O)_2\{\kappa^2N[B(CN)_4]\}_2]$. As for **1**, single crystals of **2** were obtained by slow evaporation of water off a saturated solution of **2** at room temperature after removing excess iron powder with the aid of a bar magnet. $[Fe(H_2O)_2\{\kappa^2NB(CN)_4]\}_2]$ crystallizes isotypically to $[Mn(H_2O)_2\{\kappa^2N[B(CN)_4]\}_2]$,[12] $[Co(H_2O)_2\{\kappa^2N[B(CN)_4]\}_2]$,[13] $[Mg(H_2O)_2\{\kappa^2N[B(CN)_4]\}_2]$,[23] and

dx.doi.org/10.1021/ic102278z |*Inorg. Chem.* 2011, 50, 4313–4321

Table 4. Selected Bond Angles (deg) within $[Fe(H_2O)_6][B(CN)_4]_3$, $[Fe(H_2O)_2\{\kappa^2N[B(CN)_4]\}_2]$, and $[Fe(DMF)_6][B(CN)_4]_2$[a]

$[Fe(H_2O)_2\{\kappa^2N[B(CN)_4]\}_2]$		$[Fe(H_2O)_6][B(CN)_4]_3$		$[Fe(DMF)_6][B(CN)_4]_2$	
atoms	angle	atoms	angle	atoms	angle
cation					
$O1-Fe1-O1^{\#1}$	180.0	$O1-Fe1-O1^{\#2}$	180.0(6)	O−Fe−O (range)	87.75(4)−92.25(4)
O1−Fe1−N1	85.15(4)	$O1-Fe1-O1^{\#3}$	90.04(2)		
$O1-Fe1-N1^{\#1}$	94.85(4)				
$N1-Fe1-N1^{\#1}$	90.410(7)				
anion					
$C-B-C_{range}$	105.5(2) −111.6(2)	$C-B-C_{range}$	107.39(4) - 111.55(4)	$C-B-C_{range}$	107.7(1)−110.6(2)
$N-C-B_{range}$	174.448(1) −177.235(1)	$N-C-B_{range}$	177.24(8) −177.28(7)	$N-C-B_{range}$	177.9(2)−178.9(2)
$N-C-B_{average}$	175.842	$N-C-B_{average}$	177.26	$N-C-B_{average}$	178.5

[a] Symmetry operations used to generate equivalent atoms: #1, $+y, -x, -z$; #2, $-y, x-y, z$; #3, $-x, -y, -z$.

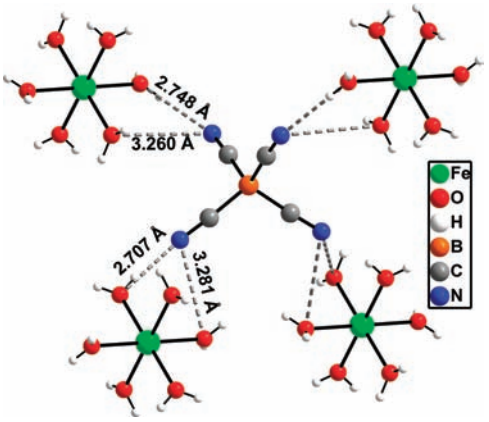

Figure 2. Environment of the $[B(CN)_4]^-$ ion in crystals of **1**. Dashed lines show the short and long distances between the donor and the aceptor atoms of the hydrogen bonds.

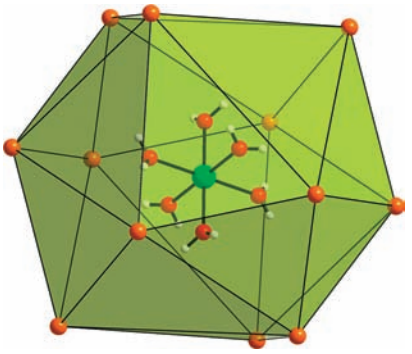

Figure 3. View of the distorted dodecahedral environment of the $[Fe(H_2O)_6]^{2+}$ ion in crystals of **1**, showing only the B atoms of the surrounding anions.

$[Zn(H_2O)_2\{\kappa^2N[B(CN)_4]\}_2]$[18] in the tetragonal space group $I\bar{4}2d$ (no. 122). The structure contains iron(II) cations, which are octahedrally coordinated by two O atoms of water molecules, trans to each other, and four N atoms of four different tetracyanidoborate anions. A view of the octahedral coordination environment of the Fe^{2+} ion with the atom-labeling scheme is given in Figure 5. With shorter Fe−O distances (2.072(1) Å) than the Fe−N distances (2.168(2) Å) the coordination sphere of the metal ion can be described as a distorted compressed octahedron with O−M−N angles deviating from 90° by ±4.85°. Two of the cyanido groups of each $[B(CN)_4]^-$ unit coordinate two neighboring Fe^{2+} ions. The result is a three-dimensional network structure of tetracyanidoborate anions bridging the iron cations, expressed by $[Fe^{II}(H_2O)_2\{\kappa^2N[B(CN)_4]\}_2]_n$ (Figure 6). This arrangement reminds of the cubic CaF_2 structure, wherein the $Fe(H_2O)_2N_4$ units replace the calcium ions and the BC_4 units occupy all tetrahedral holes. The cationic units do not form a face-centered arrangement, because every second unit is being shifted away from the face centers along the *c* axis. Therefore, the symmetry is reduced to body-centered tetragonal. The M−N and M−O bond lengths of the five tetracyanidoborates $[M(H_2O)_2\{\kappa^2N[B(CN)_4]\}_2]$ (M = Fe, Zn, Co, Mn, Mg) are compared in Table 5, which lists also the Shannon radii for the M^{2+} cations with coordination number 6. The M−O distances

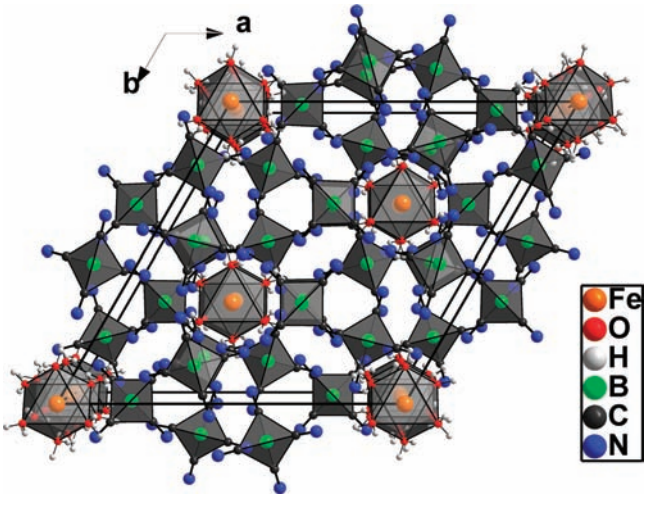

Figure 4. Arrangement of the hydrogen-bonded ions in crystals of **1** in a view along *c* of the rhombohedral unit cell.

increase in the order M = Mg, Zn, Co, Fe, to Mn as do in the same sequence the Shannon radii. This sequence is followed also roughly by the M−N distances taking into account that the X-ray structures have been measured at very different temperatures. Deviations are likely to originate from differences in specific

dx.doi.org/10.1021/ic102278z |*Inorg. Chem.* 2011, 50, 4313–4321

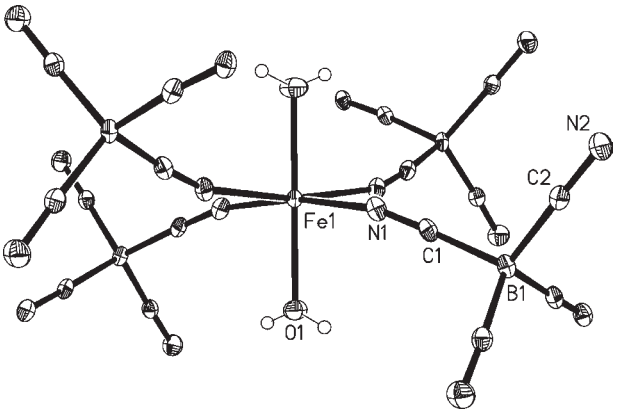

Figure 5. View of the coordination environment of the Fe^{2+} ion in $[Fe(H_2O)_2\{\kappa^2N[B(CN)_4]\}_2]$. The thermal displacement ellipsoids are drawn at the 50% probability level.

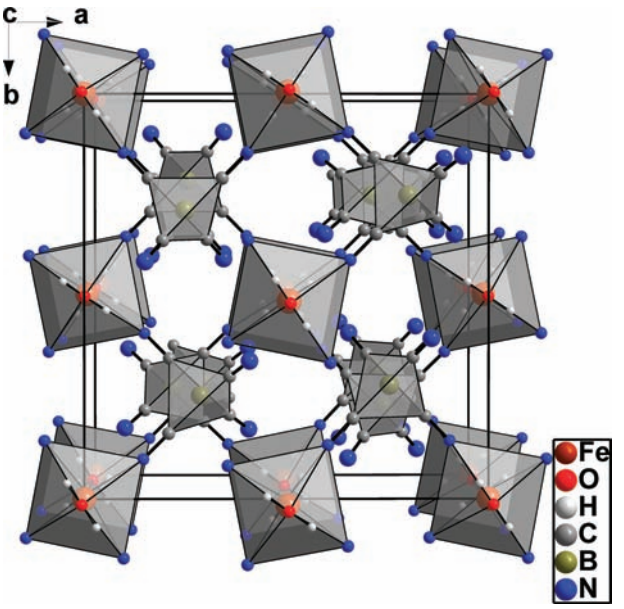

Figure 6. View of the content of the unit cell of **2** emphasizing the octahedral coordination environment of the iron ion and the tetrahedral arrangement of the anions.

coordinative bonding. These structural comparison assume the M(II) ions in the corresponding high-spin states. At least for the M = Fe case at lower temperature a transition into the low-spin state might occur, as observed for other Fe(II) compounds with a N_4O_2 coordination sphere.[25] Therefore, magnetic and Mössbauer measurements will be conducted soon in our laboratories on the title compounds. Within the $[B(CN)_4]^-$ anion two of the CN groups are bonded to the iron cation, whereas the other two are noncoordinating. Thereby, the anion is distorted from ideal tetrahedral with C−B−C angles ranging from 105.5(2)° to 111.6(2)°. This is also visible in the vibrational spectra where two different C−N absorption frequencies are observed. The C−N and B−C bond lengths in **2** are similar to those found in other tetracyanidoborates with divalent or singly charged cations.[10−15]

[Fe(DMF)$_6$][B(CN)$_4$]$_2$. Colorless single crystals of **3** were also obtained after slow evaporation of the solvent (DMF) off a saturated solution in a drybox. $[Fe(DMF)_6][B(CN)_4]_2$ crystallizes isotypically to $[Mg(DMF)_6][B(CN)_4]_2$ and $[Zn(DMF)_6][B(CN)_4]_2$[18] in the triclinic space group $P\bar{1}$ (no. 2). The structure contains isolated cations, composed of iron(II) ions, which are octahedrally surrounded by 6 molecules of dimethylformamide and isolated tetracyanidoborate anions as counterions. A view of the coordination environment of the Fe^{2+} ions as thermal ellipsoid plot with the atom-labeling scheme is given in Figure 7. The metal ion is located on a site with inversion symmetry. The Fe−O distances vary between 2.098(1) and 2.119(1) Å with O−Fe−O angles ranging from 87.75(4)° to 92.25(4)° (see Table 3 and 4). These distances and angles compare very well with those of other compounds containing $[Fe(DMF)_6]^{2+}$ octahedra, like, for example, $[Fe(DMF)_6][Sn_2I_6]$ (Fe−O 2.093−2.144 Å and O−Fe−O 86.5−93.5°).[24]

Direct coordination between the cyanido nitrogen atoms and the iron(II) ions or hydrogen bonds are not observed in **3**, but nevertheless, the tetracyanidoborate anion is distorted in this compound. The reason for the distortion could be van der Waals interactions of different strengths between the cyanido groups and the surrounding DMF molecules. The C−N and B−C bond lengths of the anion are in good agreement with other tetracyanidoborates with divalent or singly charged cations.[10,11,14,15] Figure 8 shows the arrangement of the molecular ions within the unit cell. The large complex cations are lined up along the *c* direction, and in between these rows the smaller anions are located.

Table 5. Comparison of M−N and M−O Bond Lengths (Angstroms) in $[M^{II}(H_2O)_2\{\kappa^2N[B(CN)_4]\}_2]$

bond	M = Co	M = Fe	M = Zn	M = Mn	M = Mg
M−N	2.124(2)	2.168(2)	2.145(1)	2.237(1)	2.1843(7)
M−O	2.059(2)	2.072(1)	2.055(1)	2.137(1)	2.0373(8)
Shannon radius for M^{2+}	0.745[a]	0.780[a]	0.740	0.830[a]	0.720

[a] High-spin configuration.

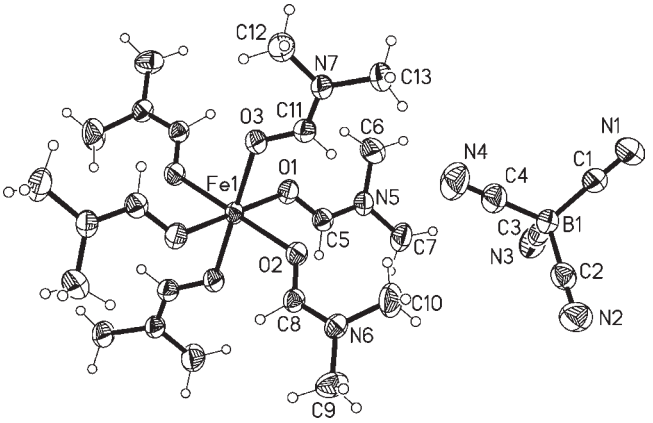

Figure 7. Molecular structure of an ion pair of **3** with atom-numbering scheme. Thermal displacement ellipsoids are drawn at the 50% probability level.

F. Solubilities. Table 6 compares the solubility of $[Fe(H_2O)_2\{\kappa^2N[B(CN)_4]\}_2]$ and $[Co(H_2O)_2\{\kappa^2N[B(CN)_4]\}_2]$ in acetone, water, and methanol. The solubility of $[Fe(H_2O)_6][B(CN)_4]_3$ in water is very high, but the compound is also soluble in acetone, acetonitrile, ethanol, methanol, and DMF. The iron(III)−tetracyanidoborate **1** is not soluble in nonpolar solvents but very soluble in polar ones, like DMF. It is likely that the

dx.doi.org/10.1021/ic102278z |*Inorg. Chem.* 2011, 50, 4313–4321

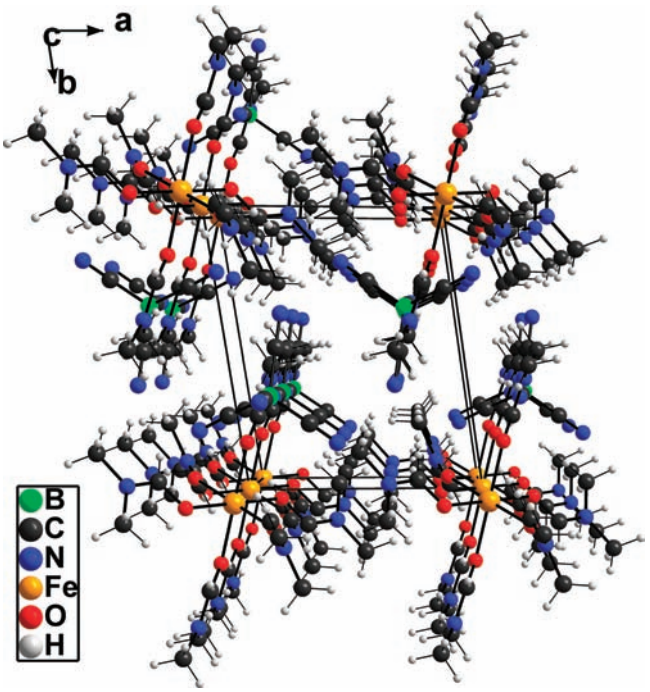

Figure 8. Arrangement of the molecular entities of **3** in the unit cell in a view along the crystallographic *c* direction.

Table 6. Solubilities (in g·L^{-1}) of Iron(II)− and Cobalt(II)−tetracyanidoborate in Different Solvents

compound	water	acetone	methanol
$[Co(H_2O)_2\{\kappa^2N[B(CN)_4]\}_2]$	9.5	20.4	21.1
$[Fe(H_2O)_2\{\kappa^2N[B(CN)_4]\}_2]$	6.9	17.5	19.3

DMF adduct is formed by dissolving $[Fe(H_2O)_6][B(CN)_4]_3$ in DMF. $[Fe(DMF)_6][B(CN)_4]_2$ is the first transition metal−tetracyanidoborate, which has a very high solubility in nonpolar solvents like dichloromethane.[15] It is also soluble in tetrahydrofurane and water. In diethyl ether oxidation of the title compound could be observed if the system is handled in air. All title compounds are not soluble in hexane.

The water-free compound **3**, which is very soluble in nonpolar solvents and contains Fe^{2+} ions and weakly bonded (solvent) ligands, is certainly a good candidate for organometallic chemistry. This aspect will be pursued in our laboratories in the future.

AUTHOR INFORMATION

Corresponding Author

*E-mail: Martin.Koeckerling@uni-rostock.de.

ACKNOWLEDGMENT

Support from the Deutsche Forschungsgemeinschaft (SPP 1191) is gratefully acknowledged. We thank Prof. Dr. H. Reincke, Dr. A. Wulff, Prof. Dr. R. Ludwig, Dr. T. Peppel, Dr. T. Küppers, Dr. Damir A. Safin, and Dipl.-Chem. A. Bernsdorf for all their valuable support.

REFERENCES

(1) Wittig, G.; Raff, P. *Z. Naturforsch.* **1951**, *6b*, 225–226.

(2) (a) Bernhardt, E.; Henkel, G.; Willner, H. *Z. Anorg. Allg. Chem.* **2000**, *626*, 560–568. (b) Williams, D.; Pleune, B.; Kouvetakis, J.; Williams, M. D.; Andersen, R. A. *J. Am. Chem. Soc.* **2000**, *122*, 7735–7741.

(3) An earlier publication reports about the structures of $Ag[B(CN)_4]$ and $Cu[B(CN)_4]$ derived from X-ray powder diffraction measurements;(a) Bessler, E.; Goubeau, J. *Z. Anorg. Allg. Chem.* **1967**, *352*, 67–76. (b) Bessler, E. *Z. Anorg. Allg. Chem.* **1977**, *430*, 38–42, but these compounds were later shown to be isocyanides, see ref (2).

(4) Bernhardt, E.; Finze, M.; Willner, H. *Z. Anorg. Allg. Chem.* **2003**, *629*, 1229–1234.

(5) (a) Bernhardt, E.; Finze, M.; Willner, H.; Lehmann, C. W.; Aubke, F. *Angew. Chem.* **2003**, *115*, 2123–2125. (b) Wilson, W. W.; Vij, A.; Vij, V.; Bernhardt, E.; Christe, K. O. *Chem.—Eur. J.* **2003**, *9*, 2840–2844.

(6) (a) Kuhlmann, M. L.; Yao, H.; Rauchfuss, T. B. *Chem. Commun.* **2004**, 1370–1371; (b) Bernhardt, E.; Berkei, M.; Willner, H.; Schürmann, M. *Z. Anorg. Allg. Chem.* **2003**, *629*, 677–685; (c) Bernhardt, E.; Henkel, G.; Willner, H.; Pawelke, G.; Bürger, H. *Chem.—Eur. J.* **2001**, *7*, 4696–4705; (d) WelzBiermann, U.; Ignatiev, N. V.; Bernhardt, E.; Finze, M.; Willner, H. WO patent 072089, 2004; (e) Hamilton, B. H.; Ziegler, C. J. *Chem. Commun.* **2002**, 842–843; (f) Finze, M.; Bernhardt, E.; Terheiden, A.; Berkei, M.; Willner, H.; Christen, D.; Oberhammer, H.; Aubke, F. *J. Am. Chem. Soc.* **2002**, *124*, 15385–15398; (g) Terheiden, A.; Bernhardt, E.; Willner, H.; Aubke, F. *Angew. Chem.* **2002**, *114*, 823–825; *Angew. Chem., Int. Ed.* **2002**, *41*, 799–801.

(7) Bernsdorf, A.; Brand, H.; Hellmann, R.; Köckerling, M.; Schulz, A.; Villinger, A.; Voss, C. *J. Am. Chem. Soc.* **2009**, *131*, 8958–8970.

(8) (a) Welz-Biermann, U.; Ignatiev, N. V.; Bernhardt, E.; Finze, M.; Willner, H. Merck Patent GmbH, Darmstadt, WO 2004/ 072089 Al, 2004. (b) Ignatiev, N. V.; Welz-Biermann, U.; Kuchceryna, A.; Bissky, G.; Willner, H. *J. Fluorine Chem.* **2005**, *126*, 1150–1159. (c) Kuang, D.; Wang, P.; Ito, S.; Zakeeruddin, S. M.; Grätzel, M. *J. Am. Chem. Soc.* **2006**, *128*, 7732–7733. (d) Bai, Y.; Cao, Y.; Zhang, J.; Wang, M.; Li, R.; Wang, P.; Zakeeruddin, S. M.; Grätzel, M. *Nat. Mater.* **2008**, *7*, 626–630 and references cited therein. (e) Shi, D.; Cao, Y.; Pootrakulchote, N.; Yi, Z.; Xu, M.; Zakeeruddin, S. M.; Grätzel, M.; Wang, P. *J. Phys. Chem. C* **2008**, *112*, 17478–17485. (f) Shi, D.; Pootrakulchote, N.; Li, R.; Guo, J.; Wang, Y.; Zakeeruddin, S. M.; Grätzel, M.; Wang, P. *J. Phys. Chem. C* **2008**, *112*, 17046–17050. (g) Xu, M.; Wenger, S.; Bala, H.; Shi, D.; Li, R.; Zhou, Y.; Zakeeruddin, S. M.; Grätzel, M.; Wang, P. *J. Phys. Chem. C* **2009**, *113*, 2966–2973.

(9) (a) Izák, P.; Köckerling, M.; Kragl, U. *Green Chem.* **2006**, *8*, 947–948. (b) Izák, P.; Köckerling, M.; Kragl, U. *Desalination* **2006**, *199*, 96–98. (c) Izák, P.; Friess, K.; Hynek, V.; Ruth, W.; Fei, Z.; Dyson, J. P.; Kragl, U. *Desalination* **2009**, *241*, 182–187. (d) Izák, P.; Ruth, W.; Fei, Z.; Dyson, P. J.; Kragl, U. *Chem. Eng. J.* **2008**, *139*, 318–321.

(10) (a) Berkei, M.; Bernhardt, E.; Schürmann, M.; Mehring, M.; Willner, H. *Z. Anorg. Allg. Chem.* **2002**, *628*, 1734–1740. (b) Küppers, T.; Bernhardt, E.; Willner, H.; Rohm, H. W.; Köckerling, M. *Inorg. Chem.* **2005**, *44*, 1015–1022. (c) Neukirch, M.; Tragl, S.; Meyer, H. J.; Küppers, T.; Willner, H. *Z. Anorg. Allg. Chem.* **2006**, *632*, 939–944. (d) Finze, M.; Bernhardt, E.; Berkei, M.; Willner, H.; Hung, J.; Waymouth, R. M. *Organometallics* **2005**, *24*, 2103–5109.

(11) Küppers, T.; Bernhardt, E.; Lehmann, C. W.; Willner, H. *Z. Anorg. Allg. Chem.* **2007**, *633*, 1666–1672.

(12) Neukirch, M. Dissertation, University of Tübingen, 2007.

(13) Nitschke, C.; Köckerling, M. *Z. Anorg. Allg. Chem.* **2009**, *635*, 503–507.

(14) Flemming, A.; Hoffmann, M.; Köckerling, M. *Z. Anorg. Allg. Chem.* **2010**, *636*, 562–568.

(15) Bernsdorf, A.; Köckerling, M. *Eur. J. Inorg. Chem.* **2009** 4547–4553.

(16) *Apex-2, v. 1.6-8, Saint, v. 6.25, SADABS-Software for the CCD detector System*; Bruker-Nonius Inc.:

(17) (a) Sheldrick, G. M. *SHELX97-Programs for crystal structure analysis* (Release 97−2); University of Göttingen: Göttingen, Germany, 1997. (b) Sheldrick, G. M. *Acta Crystallogr., Sect. A* **2008**, *64*, 112–122.

(18) Nitschke, C.; Köckerling, M. Unpublished results.
(19) Piper, T. S.; Rochow, E. G. *J. Am. Chem. Soc.* **1954**, *76*, 4318–4320.
(20) In *CRC Handbook of Chemistry and Physics*, 65th ed.; Weast, R. C., Ed.; CRC Press Inc.: Boca Raton, FL, 1985; D-156.
(21) (a) Spundflasche, E.; Fink, H.; Seifert, H. J. *Z. Anorg. Allg. Chem.* **1989**, *579*, 143–148. (b) Buchanan, D. R.; Harris, P. M. *Acta Cryst. B* **1968**, *24*, 954–960.
(22) (a) Fischer, A. *Acta Crystallogr.* **2006**, *E62*, i94–i95. (b) Hair, N. J.; Beattie, J. K. *Inorg. Chem.* **1977**, *16*, 245–250.
(23) Küppers, T.; Willner, H.; Köckerling, M. Unpublished results.
(24) Lode, C.; Krautscheid, H. *Z. Anorg. Allg. Chem.* **2000**, *626*, 326–331.
(25) See, for example: (a) Weber, B.; Kaps, E.; Weiga, J.; Achterhold, K.; Parak, F G. *Inorg. Chem.* **2008**, *47*, 487–496.(b) Blakesley, D. W.; Payne, S. C.; Hagen, K. S. **2000**, *39*, 1979−1989.